

Journal of Materials Chemistry B

Accepted Manuscript



This is an *Accepted Manuscript*, which has been through the Royal Society of Chemistry peer review process and has been accepted for publication.

Accepted Manuscripts are published online shortly after acceptance, before technical editing, formatting and proof reading. Using this free service, authors can make their results available to the community, in citable form, before we publish the edited article. We will replace this *Accepted Manuscript* with the edited and formatted *Advance Article* as soon as it is available.

You can find more information about *Accepted Manuscripts* in the [Information for Authors](#).

Please note that technical editing may introduce minor changes to the text and/or graphics, which may alter content. The journal's standard [Terms & Conditions](#) and the [Ethical guidelines](#) still apply. In no event shall the Royal Society of Chemistry be held responsible for any errors or omissions in this *Accepted Manuscript* or any consequences arising from the use of any information it contains.

ARTICLE

Copolymerization of an indazole ligand into the self-polymerization of dopamine for enhanced binding with metal ions

FCite this: DOI: 10.1039/x0xx00000x

Ka Wai Fan,^a Justine J. Roberts,^b Penny J. Martens,^b Martina H. Stenzel,^c and Anthony M. Granville*^a

5,6-dihydroxy-1*H*-indazole (DHI) is able to self-polymerize through the same mussel-inspired chemistry responsible for generating poly(dopamine) (PDA), demonstrating the potential to expand this class of catecholamine-exclusive chemistry onto heterocyclic catechol derivatives for the preparation of functional materials. Although DHI exhibits slower polymerization kinetics compared to dopamine, the two chemical species are compatibly polymerizable under the same reaction conditions and allow the preparation of copolymer coatings in different molar ratios. Of these copolymers, the 1:3-copolymer (DHI-to-dopamine ratio) has demonstrated adequate structural stability as a polymer coating. While PDA performs as an intact framework, the incorporated DHI enhances the colloidal stability and provides additional coordinating functionality through the pyrazole moieties. The 1:3-copolymer was fabricated into polymer capsules which exhibit negligible cytotoxicity towards murine dermal fibroblasts (L929) and enhanced binding behaviour towards copper(II). This represents a new channel for fabricating cargo carriers for biomedical applications that involve the use of transition metal-based species.

Received 00th January 2012,
Accepted 00th January 2012

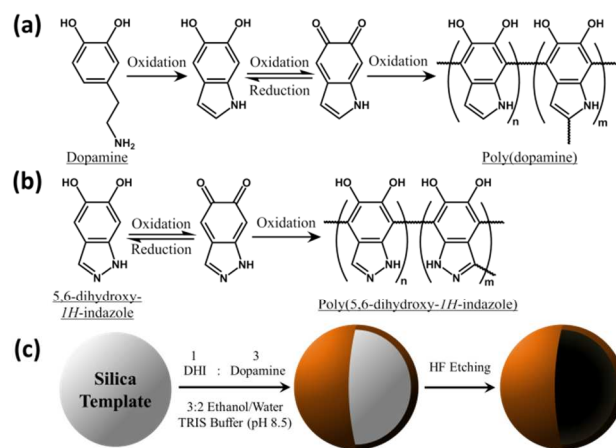
DOI: 10.1039/x0xx00000x

www.rsc.org/MaterialsB

Introduction

Poly(dopamine) (PDA) has stimulated a vast amount of research based on the mussel-inspired chemistry since it was first reported by Lee *et al.*¹ PDA is highly expressed in catechol and amino functionalities that mimic the structure of the adhesive protein of mussels and allow the polymer to coat on virtually any material with different shapes and geometries. The coated surface is chemically versatile and capable of secondary modifications, which makes PDA an ideal surface-functionalizing agent for a range of applications in membrane operation/pollution treatment,²⁻⁵ microfluidics,⁶ micropatterning,⁷⁻⁹ and the preparation of polymer brushes.¹⁰⁻¹² PDA coatings also serve as versatile platforms for substrate encapsulation.¹³⁻¹⁵ PDA-coated substrates have actively been researched of late for biomedical applications due to a host of desirable properties of this biomimetic polymer,¹⁶⁻²⁰ including negligible cytotoxicity. Removal of the substrates, *e.g.* silica particles, renders facile preparation of PDA-based surface-functional polymeric capsules.²¹⁻²⁴

Through the aqueous-based redox-facilitated self-polymerization technique, novel materials have been prepared from a range of monomers, such as norepinephrine^{25,26}, L-3,4-dihydroxyphenylalanine (L-DOPA),^{27,28} other synthetic dopamine derivatives,²⁹⁻³⁴ as well as pyrogallol and natural polyphenol compounds,³⁵ which demonstrated additional functionalities over PDA. These monomers share the same catecholamine structure with the ability to form a quinone intermediate and the subsequent



Scheme 1 Polymerization of dopamine (a) and DHI (b), and preparation of hollow capsules from the copolymer (c).

cyclized dopamine – 5,6-dihydroxy-indole (DHI_n) – when oxidized.³⁶⁻³⁸ Further oxidation activates the C-4, C-7 and, to a lesser extent, C-2 positions to form the mildly cross-linked, base structure of PDA (Scheme 1a).³⁹

Inspired by the structure of DHI_n, we recognized an opportunity to diverge the development of mussel-inspired self-polymerization by substituting dopamine/DHI_n with other heterocyclic catechol derivatives which are also capable to form an activated quinone structure *via* the mussel-inspired chemistry. The catecholic indazole

– 5,6-dihydroxy-*1H*-indazole (DHI) – is of substantial interest because of its pyrazole fused ring, which provides a permanent coordination site, *i.e.* the tertiary amine, in contrast to the pyrrole fused ring of DHI. ⁴⁰⁻⁴² Whereas no indazole-based homopolymer has been prepared previously by this self-polymerization process, our group has recently demonstrated a proof-of-concept by integrating a monohydroxy-substituted indazole into the structure of PDA as a chain terminator. ⁴³ DHI is an even better prospective candidate for self-polymerization, because of the integrated catechol functionality making it capable of behaving as dopamine/DHI (Scheme 1b).

Herein, we report the self-polymerization of DHI based on the mussel-inspired chemistry. In addition to the homopolymer formation, copolymerization has been proven achievable with mixtures of DHI and dopamine in various molar ratios. The copolymers represent the opportunity to incorporate specific coordination sites, *i.e.* the pyrazole ring, into the structure of PDA and extend the availability of ligands beyond the catechol group. ⁴⁴⁻⁴⁶ Moreover, the incorporation of the pyrazole moieties was achieved through the reaction between DHI and dopamine during the copolymerization without the need of additional post-polymerization modifications. The integrated DHI still has the catechol group available to perform binding *via* conventional conjugation as reported in literatures. ⁴⁷⁻⁴⁹ However, ultimately, the additional coordination sites are integrated to prepare novel materials for biomedical applications which can bind and deliver metal complexes which have a high affinity to nitrogen-based ligands and use as therapeutics. ⁵⁰⁻⁵⁵ For instance, copper(II) complexes prepared from the radioisotope copper-64 have been studied extensively as theranostics for targeted radiotherapy of cancer and positron emission tomography imaging. ⁵⁶⁻⁵⁹ To this end, we used copper(II) sulfate as a readily accessible and affordable model to demonstrate the enhanced binding ability over PDA with one of the DHI/dopamine copolymers in the form of stable polymeric capsules. We were also able to demonstrate that the incorporation of DHI has negligible impact on the cytotoxicity of PDA.

Experimental

Materials

Boron tribromide (BBr₃) solution, dopamine hydrochloride, tris(hydroxymethyl)aminomethane (TRIS, ≥99.8%), Dulbecco's phosphate buffered saline (DPBS), and hydrofluoric acid (48%) were purchased from Sigma Aldrich. Aerosil® OX 50 fumed silica particles were purchased from Evonik. Sodium hydrogen carbonate, magnesium sulfate (dried), copper(II) sulfate pentahydrate, and ethyl acetate were purchased from Ajax Finechem Pty Ltd. Ethanol (95%) was purchased from VWR International. Dichloromethane (stabilized with amylene) was purchased from Chem-Supply Pty Ltd. Deionized water was obtained from a Milli-Q water deionizing unit. All chemicals and solvents were used as received unless specified otherwise.

5,6-dihydroxy-1H-indazole (DHI) monomer synthesis

The DHI monomer was synthesized by demethylating 5,6-dimethoxy-*1H*-indazole according to the procedure adapted from

Schumann *et al.* ⁶⁰ in consideration of the reagent ratio suggested by Vickery *et al.* ⁶¹ Detailed procedures for the syntheses of precursor compounds are referenced in the Supplementary Information. A solution of 5,6-dimethoxy-*1H*-indazole (1 g, 5.61 mmol) in dichloromethane (17.2 mL) was chilled over an ice-water bath with a nitrogen blanket applied on top. A solution of boron tribromide (1.0 M in dichloromethane, 18.5 mL, 18.5 mmol) was added dropwise to the reaction mixture. The vessel was then capped and the reaction mixture was stirred at room temperature for 4 h. Upon completion, the vessel was submerged in an ice bath and deionized water was carefully added to the reaction mixture until the bubbling ceased. The mixture was then neutralized by the slow addition of saturated sodium hydrogen carbonate solution. The resulting mixture was extracted with dichloromethane, and the aqueous phase was collected. The product was extracted from the collected aqueous phase with ethyl acetate. The organic phase was combined and dried over anhydrous magnesium sulfate. Solvent was removed under reduced pressure. The reddish orange residue was heated in boiling deionized water for 30 min and allowed to cool to room temperature afterwards. The resulting dull yellow product was collected with a yield of 74% after drying. δ_{H} (300 MHz; DMSO-*d*₆; Me₄Si) 7.03 (1 H, s, Ar H), 7.58 (1 H, s, Ar H), 8.72 (1 H, s, CH). δ_{C} (75 MHz; DMSO-*d*₆; Me₄Si) 113.8 (C-4), 114.9 (C-9), 119.2 (C-7), 122.8 (C-8), 145.6 (C-6), 150.4 (C-5), 159.9 (C-3).

Preparation of coated silica particles and polymeric capsules

Polymer coating was performed on silica particle templates according to the procedure adapted from Peterson *et al.*, ⁴³ Postma *et al.*, ⁶² and Yu *et al.* ⁶³ with some modifications. A buffer solution of pH 9-10 was prepared by dissolving tris(hydroxymethyl)aminomethane (TRIS, 242.3 mg, 2.00 mmol) in deionized water (120 mL). Silica nanoparticles (500 mg) were dispersed in the buffer solution by sonication. DHI (75.1 mg, 0.50 mmol) was first dissolved in ethanol (95%, 80 mL) and added to the suspension, followed by the addition of dopamine hydrochloride (284.5 mg, 1.50 mmol) to obtain a reaction mixture with a pH of about 8.5. The mixture was stirred at room temperature for 24 h. Upon completion, the copolymer-coated particles were separated from the other free-floating materials by centrifuging at 3,000 rpm for 5 min. The supernatant was decanted and the particles were redispersed in fresh water. The procedure was repeated until the supernatant became clear and colorless. The particles were then collected by Millipore filtration and rinsed with several portions of deionized water. The collected particles were dried at 40 °C in vacuum oven overnight. Coated particles were also synthesized by polymerizing only dopamine (379.3 mg, 2.00 mmol) in the presence of silica templates in aqueous TRIS buffer. Similar procedures were performed to synthesize the copolymers of DHI and dopamine in 1:1 and 1:3 molar ratios (1:1-copolymer and 1:3-copolymer respectively, See Supplementary Information).

To obtain capsules of the copolymer and PDA, the coated particles were suspended in diluted hydrofluoric acid (5% v/v). The mixture was stirred at room temperature overnight to ensure the silica core was completely etched away. The resulting polymer capsules were collected by Millipore filtration, followed by rinsing with large portions of deionized water until the filtrate was neutral. The

collected capsules were purified by redispersing in deionized water and dialyzed against DPBS solution (once per 24 h for two days), and then against deionized water (once per 24 h for one day). The purified capsules were retrieved by lyophilization.

Monitoring of DHI self-polymerization

A small volume of the reaction mixture (16 μL) containing 10 mM of DHI and TRIS, respectively, was sampled at the designated time (1, 6, 10, 14, 24, 28, 48, 66.5 and 88 h). The aliquot was then transfer to a quartz cuvette and diluted with 3:2 water/ethanol mixture (3 mL). The absorbance of the prepared sample was measured between 700 and 200 nm with a UV-Vis spectrophotometer using blank water/ethanol mixture for baseline correction prior to each measurement.

Cell growth inhibition study of polymeric capsules

The buffer (PBS, Sigma D5652) and medium (DMEM, Sigma D5523) used have an initial pH of 7.4, but the change in pH was not monitored over the duration of the study. The cell culture medium was prepared with DMEM solution which contained fetal bovine serum (10%, Moregate Australia New Zealand) and penicillin-streptomycin (1%, Sigma 4458). The polymeric capsule samples were analyzed using a growth inhibition assay with murine dermal fibroblasts (L929) (ISO 10993-5 procedure). 5×10^4 fibroblasts $\cdot\text{mL}^{-1}$ were seeded onto 35-mm diameter tissue culture dishes. After 24 h of incubation at 37 $^{\circ}\text{C}$ in a 5%- CO_2 humidified atmosphere, the media was discarded and 1 mL of sample solution was added to the cells. The sample solution was prepared by first extracting 4 mg of polymeric capsule sample $\cdot\text{mL}^{-1}$ of media, or media alone (positive control) for 48 h at 37 $^{\circ}\text{C}$. The extracted solution, 1 mL, was added to 3 mL of media, sterile filtered and 1 mL of this extract solution was added to the cells. Negative controls were also prepared with 4%, 5%, or 7.5% ethanol (EtOH) in cell culture media. Following an additional 48 h of incubation, the cells were trypsinized, and counted with a cell viability analyzer (Vi-cell XR, Beckman Coulter).

Copper(II) binding trial on coated particles

The coated particles (8.00 mg) were dispersed in a solution of copper(II) sulfate pentahydrate (100 mL, 10 mM, pH 5) and stirred overnight. The treated particles were collected by Millipore filtration and rinsed with copious amounts of deionized water until the filtrate was clear and colorless. The collected particles were dried under vacuum.

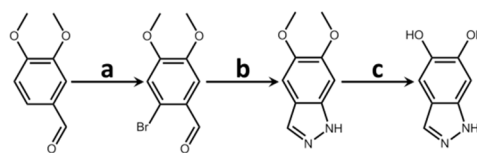
Characterization

^1H , ^{13}C and 2D nuclear magnetic resonance (NMR) spectroscopies were performed on a Bruker Avance III 300 MHz spectrometer equipped with a SampleXpress automatic sample changer and BBFO z-gradient probe. ^{13}C solid-state (CP-MAS) spectroscopy was performed on a Bruker Avance III 300 Solid State spectrometer equipped with a 4 mm 1H/X broadband CP-MAS (cross polarization-magic angle spinning) probe. Ultraviolet-visible (UV-Vis) spectroscopy was performed on a Varian Cary 300 UV-Visible Spectrophotometer using deionized water as the solvent/dispersant unless stated otherwise. Attenuated total reflectance Fourier transform infrared (ATR-FTIR) spectroscopy was performed on a

Bruker IFS 66/S single-beam spectrometer. Gel permeation chromatography (GPC) was performed by a unit purchased from Shimadzu Scientific Instruments, which included a SIL-10AD VP auto-sampler, a LC-20AT pump (set at 1 $\text{mL} \cdot \text{min}^{-1}$), a CTO-10A VP column oven (set at 50 $^{\circ}\text{C}$), and a RID-10A refractive index (RI) detector. The chromatography columns (Phenogel – 10^5 , 10^4 and 10^3 \AA pore size) were purchased from Phenomenex. *N,N*-dimethylacetamide (DMAc) was employed as the mobile phase. Dynamic light scattering (DLS) and zeta potential measurements were performed on a Malvern Zetasizer Nano using deionized water as the dispersant unless specified. Thermogravimetric analysis (TGA) was performed using a Q5000 (V3.15 Build 263) instrument purchased from TA Instruments. Transmission electron microscopy (TEM) images were acquired with a JEOL 1400 transmission electron microscope. Scanning electron microscopy (SEM) images were acquired with a Nova NanoSEM 230 field-emission scanning electron microscope. Energy dispersive X-ray spectroscopy (EDS) was performed using a FEI Tecnai G2 20 transmission electron microscope. Laser scanning confocal microscopy (LSCM) was performed on a Zeiss LSM780 confocal microscope.

Results and discussion

The synthesis of DHI has rarely been reported in the literature. As a result, we developed a straightforward, three-step reaction sequence (Scheme 2) to obtain this essential monomer with an adequate yield and high purity (See NMR spectra from Fig. S1, S2). The molecular structure of DHI has been studied through 2D NMR (Fig.S3) in order to identify the corresponding sites – C-3, 4 and 7 – which would potentially be reactive during the self-polymerization. In contrast to DHI, the 2-position of DHI is substituted with a tertiary amine. While C-3 may still be available for reactions, its ability for cross-linking is significantly lower because of the resulting steric hindrance as the self-polymerization proceeds. The consequence of this structural difference will be elaborated more in later discussion.



Scheme 2 Synthesis of 5,6-dihydroxy-1H-indazole: (a) bromine, chloroform, reflux at 60 $^{\circ}\text{C}$ overnight; (b) hydrazine monohydrate, 1,4-dioxane, reflux at 80 $^{\circ}\text{C}$ overnight; (c) boron tribromide, dichloromethane, room temperature for 4 hours.

Despite the seemingly comparable hydrophilic nature to DHI, as deduced from the molecular structure, the DHI monomer exhibits much lower water-solubility. As a result, a solvent mixture of water and ethanol in optimized ratio (3:2 v/v) was used as the reaction medium. The use of ethanol does not only aid the dissolution of DHI, but also retains the “green” motif of the mussel-inspired chemistry. It is notable that the use of water/ethanol mixture did not affect the self-polymerization of dopamine. DHI self-polymerized at ambient conditions and showed a progressive change in color from amber yellow to dark brown as the homopolymer – PDHI – was

formed (Fig. 1a). Similar phenomenon was observed during the preparation of the 1:1- and 1:3-copolymer (Fig. S4).

The temporal change in UV-Vis absorbance for the reaction mixture was monitored over an 88-hour period. As illustrated by Fig. 1b, the spectra exhibited significant changes at wavelengths below 450 nm. For instance, the dominant absorption peak at 366 nm displayed a slight blue-shift and reduction in intensity throughout the course of the polymerization. This absorption peak is speculated to originate from changes in the aromaticity of the pyrazole functionality of DHI due to the catechol group. This influence could be due to both polymerization leading to aromaticity changes, or quinone formation from both monomers and polymers. The observed linear decrease in intensity at 366 nm (Fig. 2a), therefore, indicates that these changes in aromaticity are occurring throughout the entire 88-hour period.

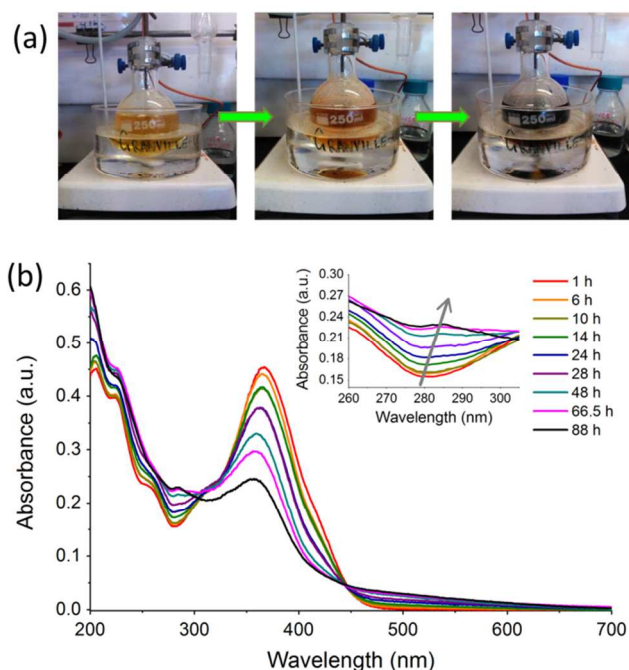


Fig. 1 Progress of the self-polymerization of DHI (a) and the spectral change of the reaction mixture monitored by UV-Vis spectrophotometry over 88 h (b). The inset emphasizes on the increasing absorbance at 260-305 nm over the course of the reaction.

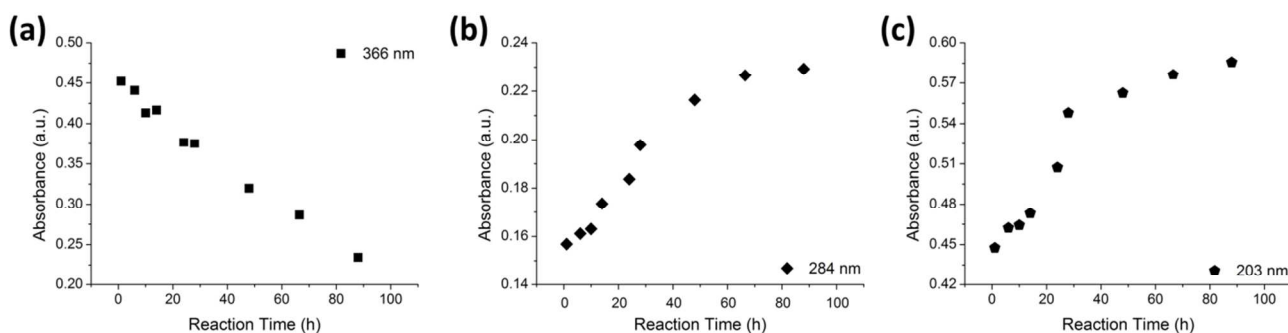


Fig. 2 The change in absorbance of the self-polymerizing DHI at 366 nm (a), 284 nm (b) and 203 nm (c) monitored by UV-Vis spectrophotometry over 88 hours.

In contrast to the peak at 366 nm, the spectral changes from 200-300 nm are characteristic for the formation of materials similar to melanin, which in turn hint on the structure of PDHI.⁶⁴ Gradual increase in absorbance is observed at 284 nm (Fig. 2b) and 203 nm (Fig. 2c), respectively. Both trends approached a plateau before the end of the 88-hour period, indicating that the PDHI – a melanin analogue – had reached a stable structure, *i.e.* relatively minor increases to particle size or surface coating thickness. Therefore, this suggests that while the aromaticity of monomers and polymers in the system is still in flux during the reaction time, the melanin-like polymer being formed has predominantly finished in roughly 40 h. In brief, the UV-Vis kinetics results indicate that the self-polymerization of DHI proceeds at a significantly slower rate than that reported for dopamine.²⁴

¹³C solid-state NMR (CP-MAS) spectrometry was performed to elucidate the architecture and the structural composition of PDHI, as well as the 1:1- and 1:3-copolymers (Fig. 3). Comparison was made against the spectra of the DHI monomer and PDA. Broad clusters of peaks can be observed for the spectra of polymeric samples, which indicate the architectural differences with the DHI monomer. The PDHI spectrum exhibits extensive peak-broadening at 110-130 ppm, corresponding to part of the benzene structure of DHI. While the bridging carbons, *i.e.* C-8 and C-9, are inactive by nature, the broadening effect is believed to be due to the formation of carbon-carbon bonds at C-4 and C-7. The result suggests that PDHI consists of a π -conjugated system as illustrated in Scheme 1, which is analogous to the proposed structure of PDA.⁶⁵ The absence of the C-3 peak of DHI in all of the other spectra indicates that it is one of the reactive sites during the self-polymerization. It is suspected that the reactions at C-3 have caused the peak to shift upfield and contributed to the broadening observed at 140-155 ppm, where the unreactive catechol C-5 and C-6 are. Unlike DHI, linear/ branched structures are more likely to be developed from C-3 instead of cross-linking due to the inherent steric hindrance as depicted previously by the molecular structure of DHI (Scheme 2).

The spectra of 1:1- and 1:3-copolymer resemble that of PDA due to the high degree of overlapping in the aromatic regions, which is attributed to the high architectural similarity

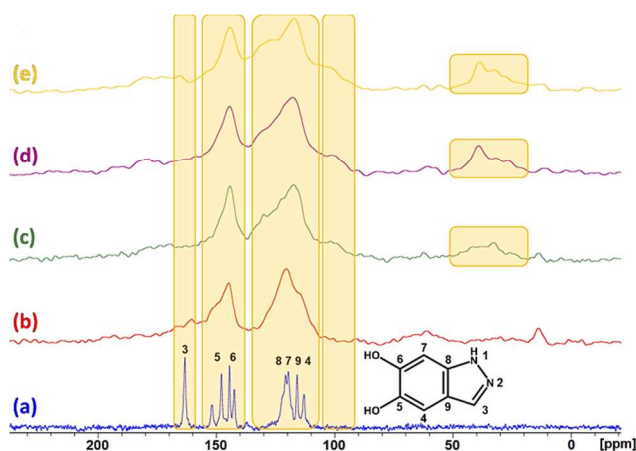


Fig. 3 Comparison of the ^{13}C solid-state NMR spectra of DHI (a), PDHI (b), 1:1-copolymer (c), 1:3-copolymer (d) and PDA (e).

between PDHI and PDA. However, peaks corresponding to the aliphatic amine of uncyclized dopamine can be located at 20-50 ppm. The peak intensity increases and the signals are sharper with the increasing dopamine content, suggesting the successful incorporation of dopamine with DHI. A similar trend is observed from the aromatic shoulder peak at 100 ppm, and also from the weak carbonyl signals of PDA at 170-190 ppm.

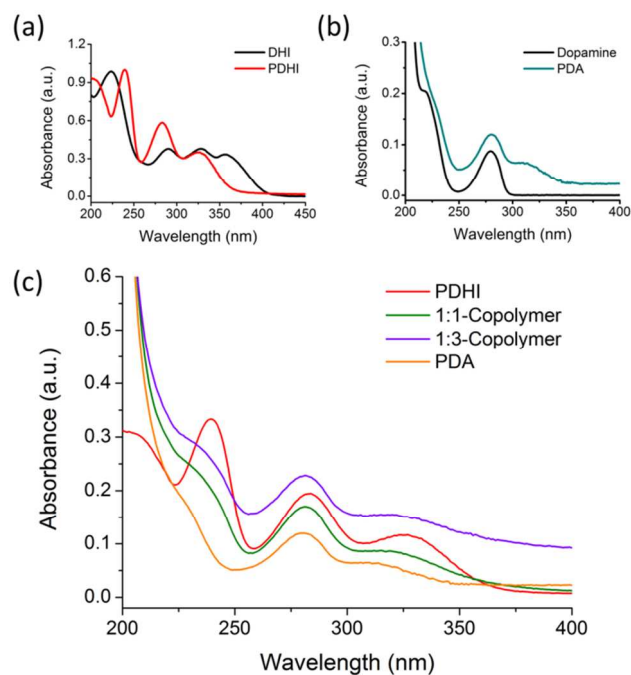


Fig. 4 Comparisons of the UV-Vis spectrum between: DHI and PDHI (a), dopamine and PDA (b), and the polymeric samples.

In addition to ^{13}C solid-state NMR, UV-Vis spectrophotometry also provides evidence to confirm the generation of new materials after the self-polymerization of DHI. The spectral features become more distinctive by using water as the dispersant for DHI and PDHI. The shifts in peak position are significant while a new peak has emerged at 325 nm (Fig. 4a), which is analogous to the spectral

change observed dopamine self-polymerized to PDA (Fig. 4b). Furthermore, the spectra of 1:1- and 1:3-copolymers exhibit features (at 231, 281 and 318 nm) analogous to those in PDA spectra, although being red-shifted (Fig. 4c). The shift is believed to have originated from incorporating PDHI into the structure of PDA, *i.e.* copolymerization has taken place. Similar effects can be observed from the ATR-FTIR spectra of the copolymers (Fig. S5). However, the differences are less obvious due to the highly similar bonding constitution shared between PDHI and PDA.

PDHI was found to be completely soluble in DMAc, which suggested that the polymer does not exhibit the same degree of cross-linking as the highly insoluble PDA. The 1:1- and 1:3-copolymers were partially soluble in DMAc, with a soluble content of 51% and 26%, respectively, as quantified from the residual material on the syringe filter (Table S2). The solubility of the material aligns with the amount of DHI that have been incorporated - the higher the DHI content the higher the solubility. The increase in solubility indicates that the incorporation of DHI potentially lowers the cross-linking density of PDA and copolymer systems by introducing more mobile linear/branched features to the overall structure.

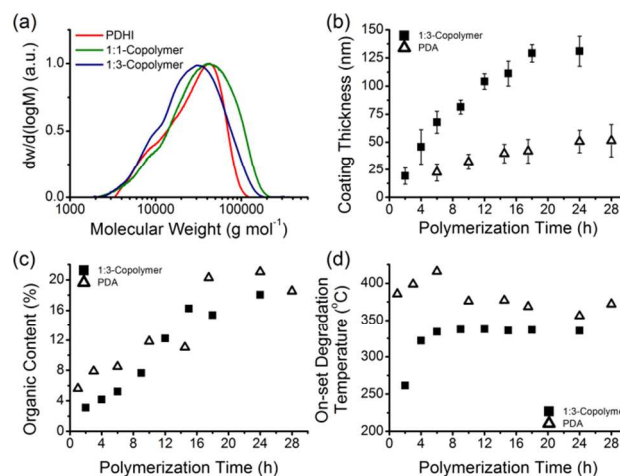


Fig. 5 Molecular weight distribution of PDHI, 1:1- and 1:3-copolymer obtained by GPC (a), and kinetics of coating thickness growth (b), increase of organic content (c) and change in on-set degradation temperature (d).

Gel permeation chromatography was performed on the soluble fractions of the synthesized materials, whereas the analysis has been proven inapplicable to PDA due to its insoluble nature. As illustrated by Fig. 5a, the molecular weight (MW) distribution of the synthesized materials skewed towards high-MW, with $M_n \approx 20,000 \text{ g mol}^{-1}$ and a broad dispersity of $D \geq 1.48$ (Table S3), which is indicative that PDHI and the copolymers are truly polymeric despite the presence of traces of oligomeric species in the samples. The high dispersity and lack of correlation between the DHI content and MW of the sample are results of the uncontrolled nature of the self-polymerization.

Being structurally similar to PDA has granted these newly prepared polymeric species the potential to perform surface coating in a simple, one-step, aqueous-based procedure. In the presence of

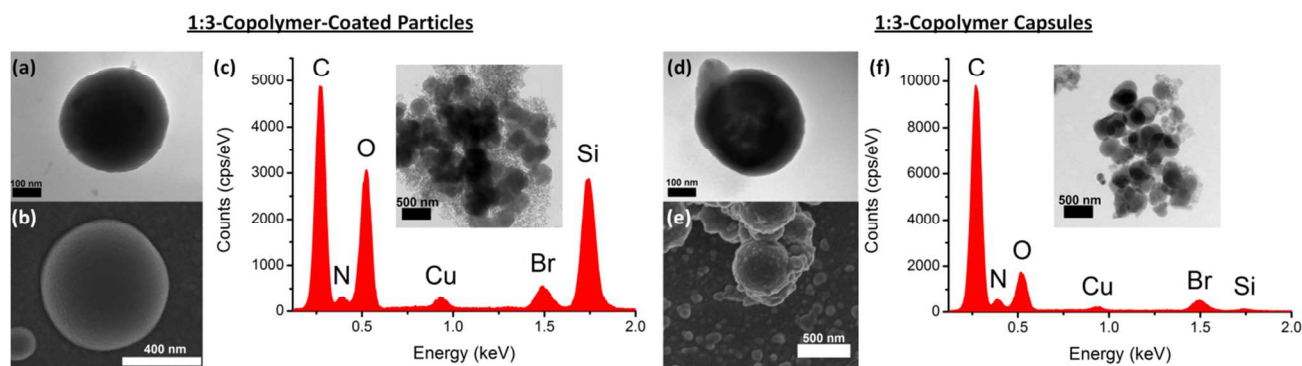


Fig. 6 Characterisations performed with TEM (a and d, scale bar = 100 nm), SEM (b and e, scale bar = 400 nm and 500 nm), and EDS (c and f) for 1:3-copolymer-coated silica particles (left) and 1:3-copolymer capsules (right), respectively. The insets illustrate the area being irradiated by X-ray during EDS analysis (scale bar = 500 nm).

silica particle templates, an *in situ* coating formed directly onto the particle surface as the self-polymerization proceeded over 24 hours. However, only the 1:3-copolymer can form a coating with comparable structural stability as PDA, while 1:1-copolymer and PDHI homopolymer were observed to delaminate from the template during the cleaning process (Fig. S6). As previously mentioned, we speculated that the DHI polymerization reduced cross-linking by introducing linear/branched structures which are more mobile. The observance of delamination and increased solubility of the generated polymer with increasing DHI content would support this finding.

Since the 1:3-copolymer is able to form the most stable coating on silica templates, the application aspect of DHI has been focused on this copolymer material. The influence of DHI on the self-polymerization kinetics of dopamine was first determined by monitoring changes to the 1:3-copolymer coating on silica particles over time. As shown by the DLS measurements, the coating thickness for the 1:3-copolymer increased more rapidly than that for PDA, while both traces plateaued within 24 hours (Fig. 5b). In contrast, the TGA result shows that both the 1:3-copolymer and PDA coatings exhibited a similar organic content which increased at the same rate and reached a maximum within 24 hours (Fig. 5c). Since thickness is correlated to volume, the 1:3-copolymer is believed to have generated a coating of lower density than PDA by embodying similar amount of material within a larger volume. The lower density of the coating is attributed to the presence of more branched structures in DHI-incorporated polymers.

The rapid establishment of high on-set degradation temperatures for the PDA kinetic samples suggests that the coating had immediately stabilized by cross-linking as the self-polymerization proceeded (Fig. 5d). The incorporation of DHI, conversely, has introduced an 8-hour induction period before establishing a measurable coating with a stable on-set degradation temperature. Since the copolymer started to degrade at lower temperatures, this material is not as thermally stable as PDA. In short, DHI has minimal influence on the self-polymerization kinetics of dopamine as a comonomer even though it has been shown to exhibit a slower polymerization rate, while it has a more significant impact on the structural properties when incorporated into PDA by lowering the density of the coating as well as the degree of cross-linking.

A more in-depth study of the 1:3-copolymer coating on silica particles was carried out with TEM and SEM (Fig. 6a and 6b). Uniform coating has been formed on the particle surface with no observable defects. The copolymer demonstrated adequate qualities as a surface coating. Afterwards, copolymer capsules (1:3, DHI-to-dopamine) were prepared by redispersing the coated particles in a 5% HF solution overnight to etch the silica core (Scheme 1c). As illustrated by the TEM image of the etched particles (Fig. 6d), the solid core seen in the coated particles no longer existed while a cavity was resulted. Similar to the coated particles, the capsules did not show any major defect. Although the kinetics study suggests the copolymer coating has a lower density than PDA, the thicker capsule wall is believed to enhance the structural integrity and prevented the capsules from collapsing as indicated by SEM images (Fig. 6e).

The elemental composition of the coated particles and capsules were analyzed by EDS. Both samples are expected to show peaks of C, N, and O. While the Cu peak originated from the copper grid, the Br peak is suspected to have originated from residual bromide during the monomer synthesis. In contrast to the spectrum of the particles (Fig. 6c), the absence of the Si peak and the substantial reduction of the O peak in the spectrum of the copolymer capsules (Fig. 6f) indicates the complete removal of the silica core. The TEM insets also reveal that the capsules are more transparent to the electron beam compared to the particles, which further proves that a hollow interior has been generated. The absence of silica was also confirmed by results acquired from TGA and ATR-FTIR for the copolymer capsules (Fig. S7). To further elucidate the hollow nature of the nanocapsules generated, LSCM was performed using Nile red as the fluorescent dye. Images in the Supporting Information illustrate the cavity being fully fluorescent and thus support the EDS-TEM data for hollow nanocapsule generation (Fig. S8).

Since occasional aggregation has been observed for both copolymer-coated particles and copolymer capsules (Fig. S9) in the dry state, the zeta potential (ζ) of these samples was measured and summarized in Table S4 to help determine the respective colloidal stability. Briefly, the two copolymer samples can be classified as moderately stable colloids due to the negative ζ values, -35.8 ± 0.2 mV for the coated particles and -42.9 ± 0.8 mV for the copolymer capsules, indicative of a low tendency for particle aggregation. PDA-coated particles and PDA capsules were also analyzed as a control

comparison, and the ζ values were found to be -32.4 ± 0.9 mV and -8.9 ± 1.3 mV, respectively. Interestingly, these results suggest that PDA capsules have the highest tendency to aggregate out of all samples. Although aggregates would still form quite readily, the incorporation of DHI has significantly enhanced the colloidal stability of the prepared polymeric capsules.

Polymeric capsules based on PDA have gained attention in the biomedical field as cargo carriers for their simple aqueous-based preparation, promising properties, and low cytotoxicity.^{62,63,66} The further functionalization of PDA capsules would widen their applications, while care must be taken to not increase their cytotoxicity. We previously found that the incorporation of 5HI at 50 mol% had no impact on PDA cytotoxicity,⁴³ whereas a polymerizable indazole, *i.e.* DHI, may elicit a different cytotoxic response. Hence, the cytocompatibility of 1:3-copolymer capsules is of immense interest for the present work. A growth inhibition assay with murine dermal fibroblasts (L929) (ISO 10993-5 procedure) was performed to investigate the cytotoxicity of 1:3-copolymer capsules, and compared to PDA capsules.

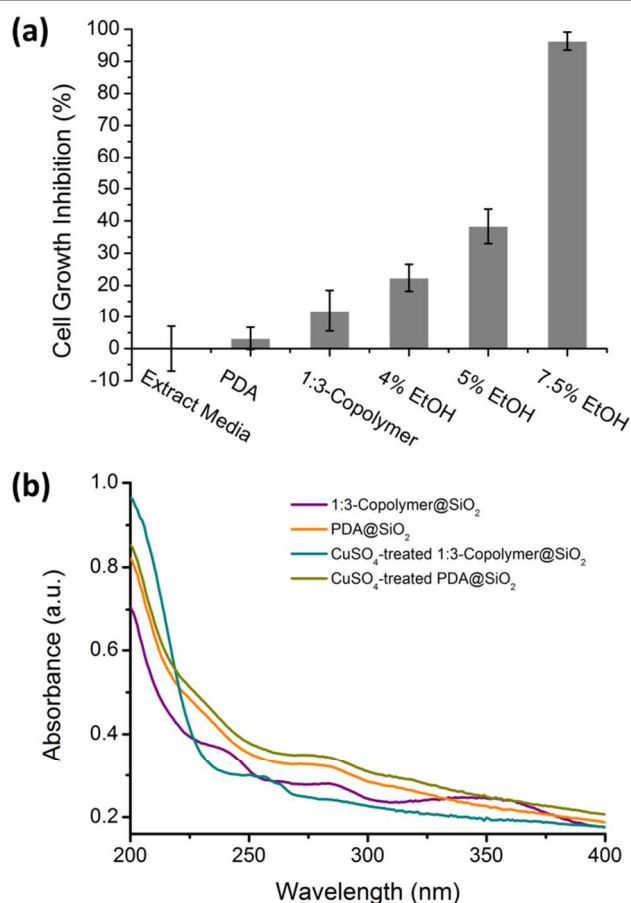


Fig. 7 Cell growth inhibition of capsules prepared from the 1:3-copolymer and PDA (a); UV-Vis results obtained from Cu(II) binding study (b).

Both 1:3-copolymer and PDA capsules are cytocompatible as evidenced by the minimal cell growth inhibition compared to extract media (Fig. 7a). Although the copolymer inhibited the growth of L929 cells to a greater extent than PDA, the level is still far below

the 30% inhibition threshold specified in the ISO 10993-5 procedure. Therefore, the copolymer capsules are not considered as cytotoxic. All ethanol negative controls show significantly higher levels of growth inhibition. The incorporation of DHI without inducing significant adverse effect on the cytotoxicity level of PDA is significantly beneficial to the potential application of the copolymer capsules as therapeutics carriers.

To demonstrate the potential of these DHI integrated capsules to bind metal-complexed therapeutics, the binding of a copper-based solution was probed as a model system. We performed a preliminary binding trial by dispersing the 1:3-copolymer and PDA samples in 10 mM copper(II) sulfate (CuSO₄) solution overnight (*ca.* 18 h). It is notable that no change in color or pH (*i.e.* stayed blue and at pH 5) has been observed after binding for both set-ups. UV-Vis analyses of the cleaned and dried samples indicate that Cu²⁺ has bound to the pyrazole moieties of 1:3-copolymer.⁶⁷ As illustrated in Fig. 7b, there are no observable changes to the PDA samples after being treated by CuSO₄ although PDA is a good copper(II) absorbant because of the catechol groups.^{68,69} In contrast, the broad absorption peaks of the 1:3-copolymer have disappeared after CuSO₄-treatment while a new peak has risen at about 260 nm. The strong absorption of CuSO₄ below 240 nm is also observed from the spectrum of the treated 1:3-copolymer (Fig. S10). The observed spectral changes were primarily attributed to the integrated DHI or, to be specific, the presence of pyrazole moieties as ligands.⁴⁰⁻⁴² It should be noted that binding of Cu²⁺ is still achievable through the catechol groups present in the 1:3-copolymer even though the change may not be detectable. Therefore the UV-Vis results of the copolymer samples suggest that further binding of Cu²⁺ can be achieved through the pyrazole rings. More binding studies with different metals will be required to gain insights of the loading efficiency and site selectivity.

Conclusions

To conclude, fabrication of novel functional materials based on mussel-inspired chemistry do not always require a monomer derived from dopamine. Heterocyclic catechol derivatives are potential monomer candidates provided that the selected compound can undergo self-polymerization in similar aqueous-based, oxidizing conditions. In our case, the compound DHI was chosen so as to incorporate a potential metal and drug binding site into the coating. Further investigation is yet to be undergone to identify the tailored applications for PDHI and 1:1-copolymer based on their unique solubility, architecture, and structural composition. On the other hand, the 1:3-copolymer has demonstrated promising properties as a surface coating material. Due to the inherent low cytotoxicity and additional ligating moieties of the copolymer capsules prepared from DHI and dopamine (1:3), future research will be focused on their potential to deliver metal-based therapeutics, in particular the uptake and release behavior.

Author Contributions

K.W.F. and J.J.R. performed experimental work and analyzed experimental results. K.W.F., J.J.R., and A.M.G. wrote the manuscript. P.J.M., M.H.S., and A.M.G. conceived and designed the project.

The authors declare no competing financial interests.

Acknowledgments

We thank Dr James M. Hook and Dr Aditya Rawal for aid in performing the solid state NMR experiments and helpful discussions of the results. The equipment in the NMR Facility at the Mark Wainwright Analytical Centre is supported by the Australian Research Council through Linkage Infrastructure, Equipment and Facilities Funding Scheme (LE0989541 and LE120100027) and the UNSW Major Research Equipment and Infrastructure Initiative (MREII). We acknowledge the support of the Electron Microscopy Unit (EMU) at Mark Wainwright Analytical Centre (UNSW Australia), especially to Ms Katie Levick for performing EDS analysis. We thank Mr Yan Jin for acquiring the SEM images of the samples. We also thank Dr Hongxu Lu for acquiring the LSCM images of the dye-loaded copolymer capsules. K.W.F. would like to acknowledge the support of the Australian Government for scholarship funding in the form of an Australian Postgraduate Award and a UNSW Engineering Research Award. J.J.R. would like to acknowledge the support of a Whitaker International Scholarship Grant.

Notes and references

^a Centre for Advanced Macromolecular Design, School of Chemical Engineering, UNSW Australia.

^b Graduate School of Biomedical Engineering, UNSW Australia.

^c Centre for Advanced Macromolecular Design, School of Chemistry, UNSW Australia.

† Electronic Supplementary Information (ESI) available: UV-Vis, ATR-FTIR, and NMR spectra, TGA thermograms and experimental procedures. See DOI: 10.1039/b000000x/

- H. Lee, S. M. Dellatore, W. M. Miller and P. B. Messersmith, *Science*, 2007, **318**, 426-430.
- Y. Xiang, F. Liu and L. Xue, *J. Membr. Sci.*, 2015, **476**, 321-329.
- Q. Liu, N. Wang, J. Caro and A. Huang, *J. Am. Chem. Soc.*, 2013, **135**, 17679-17682.
- B. D. McCloskey, H. B. Park, H. Ju, B. W. Rowe, D. J. Miller and B. D. Freeman, *J. Membr. Sci.*, 2012, **413**, 82-90.
- Z. Dong, F. Zhang, D. Wang, X. Liu and J. Jin, *J. Solid State Chem.*, 2015, **224**, 88-93.
- I. You, S. M. Kang, S. Lee, Y. O. Cho, J. B. Kim, S. B. Lee, Y. S. Nam and H. Lee, *Angew. Chem. Int. Ed.*, 2012, **51**, 6126-6130.
- Y. Wang, N. Li, D. Li, S. Yu and C. Wang, *Mater. Lett.*, 2015, **140**, 127-130.
- L. Zhang, J. Wu, M. N. Hedhili, X. Yang and P. Wang, *Journal of Materials Chemistry A*, 2015, **3**, 2844-2852.
- Y. Jin, Y. Cheng, D. Deng, C. Jiang, T. Qi, D. Yang and F. Xiao, *ACS Applied Materials & Interfaces*, 2014, **6**, 1447-1453.
- S. P. Le-Masurier, G. Gody, S. Perrier and A. M. Granville, *Polymer Chemistry*, 2014, **5**, 2816-2823.
- W. Sheng, B. Li, X. Wang, B. Dai, B. Yu, X. Jia and F. Zhou, *Chem. Sci.*, 2015, **6**, 2068-2073.
- S. P. Le-Masurier, H. T. T. Duong, C. Boyer and A. M. Granville, *Polymer Chemistry*, 2015, **6**, 2504-2511.
- M. Kohri, H. Kohma, Y. Shinoda, M. Yamauchi, S. Yagai, T. Kojima, T. Taniguchi and K. Kishikawa, *Polymer Chemistry*, 2013, **4**, 2696-2702.
- W. Wang, Y. Jiang, Y. Liao, M. Tian, H. Zou and L. Zhang, *J. Colloid Interface Sci.*, 2011, **358**, 567-574.
- L. Liu, Y. Guo, G. Odusote, F. Qu and R. D. Priestley, *ACS Applied Materials & Interfaces*, 2013, **5**, 9167-9171.
- X. Chen, Y. Yan, M. Müllner, M. P. van Koeveden, K. F. Noi, W. Zhu and F. Caruso, *Langmuir*, 2014, **30**, 2921-2925.
- J.-H. Lin, C.-J. Yu, Y.-C. Yang and W.-L. Tseng, *PCCP*, 2015, **17**, 15124-15130.
- X. Zhang, S. Wang, L. Xu, L. Feng, Y. Ji, L. Tao, S. Li and Y. Wei, *Nanoscale*, 2012, **4**, 5581-5584.
- Y. Liu, K. Ai, J. Liu, M. Deng, Y. He and L. Lu, *Adv. Mater.*, 2013, **25**, 1353-1359.
- T. Repenko, S. Fokong, L. De Laporte, D. Go, F. Kiessling, T. Lammers and A. J. C. Kuehne, *Chem. Commun.*, 2015, **51**, 6084-6087.
- L. Zhang, J. Shi, Z. Jiang, Y. Jiang, S. Qiao, J. Li, R. Wang, R. Meng, Y. Zhu and Y. Zheng, *Green Chem.*, 2011, **13**, 300-306.
- L. Zhang, J. Shi, Z. Jiang, Y. Jiang, R. Meng, Y. Zhu, Y. Liang and Y. Zheng, *ACS Applied Materials & Interfaces*, 2011, **3**, 597-605.
- J. Cui, Y. Wang, A. Postma, J. Hao, L. Hosta-Rigau and F. Caruso, *Adv. Funct. Mater.*, 2010, **20**, 1625-1631.
- H. Xu, X. Liu and D. Wang, *Chem. Mater.*, 2011, **23**, 5105-5110.
- S. Hong, J. Kim, Y. S. Na, J. Park, S. Kim, K. Singha, G.-I. Im, D.-K. Han, W. J. Kim and H. Lee, *Angew. Chem. Int. Ed.*, 2013, **52**, 9187-9191.
- S. M. Kang, J. Rho, I. S. Choi, P. B. Messersmith and H. Lee, *J. Am. Chem. Soc.*, 2009, **131**, 13224-13225.
- M. E. Lyngé, R. v. d. Westen, A. Postma and B. Stadler, *Nanoscale*, 2011, **3**, 4916-4928.
- P. Manini, M. d'Ischi and G. Prota, *The Journal of Organic Chemistry*, 2001, **66**, 5048-5053.
- M. Ambrico, P. F. Ambrico, A. Cardone, N. F. Della Vecchia, T. Ligonzo, S. R. Cicco, M. M. Talamo, A. Napolitano, V. Augelli, G. M. Farinola and M. d'Ischia, *Journal of Materials Chemistry C*, 2013, **1**, 1018-1028.
- M. Ambrico, N. F. D. Vecchia, P. F. Ambrico, A. Cardone, S. R. Cicco, T. Ligonzo, R. Avolio, A. Napolitano and M. d'Ischia, *Adv. Funct. Mater.*, 2014, **24**, 7161-7172.
- L. García-Fernández, J. Cui, C. Serrano, Z. Shafiq, R. A. Gropeanu, V. S. Miguel, J. I. Ramos, M. Wang, G. K. Auernhammer, S. Ritz, A. A. Golriz, R. Berger, M. Wagner and A. del Campo, *Adv. Mater.*, 2013, **25**, 529-533.
- Z. Shafiq, J. Cui, L. Pastor-Pérez, V. San Miguel, R. A. Gropeanu, C. Serrano and A. del Campo, *Angew. Chem.*, 2012, **124**, 4408-4411.
- A. Pezzella, A. Iadonisi, S. Valerio, L. Panzella, A. Napolitano, M. Adinolfi and M. d'Ischia, *J. Am. Chem. Soc.*, 2009, **131**, 15270-15275.
- L. Capelli, O. Crescenzi, P. Manini, A. Pezzella, V. Barone and M. d'Ischia, *The Journal of Organic Chemistry*, 2011, **76**, 4457-4466.
- S. Hong, J. Yeom, I. T. Song, S. M. Kang, H. Lee and H. Lee, *Advanced Materials Interfaces*, 2014, DOI: 10.1002/admi.201400113.
- H. Okuda, K. Wakamatsu, S. Ito and T. Sota, *The Journal of Physical Chemistry A*, 2008, **112**, 11213-11222.
- J. Liebscher, R. Mrówczyński, H. A. Scheidt, C. Filip, N. D. Hädade, R. Turcu, A. Bende and S. Beck, *Langmuir*, 2013, **29**, 10539-10548.
- M. d'Ischia, A. Napolitano and A. Pezzella, *Eur. J. Org. Chem.*, 2011, **2011**, 5501-5516.
- M. d'Ischia, A. Napolitano, A. Pezzella, P. Meredith and T. Sarna, *Angew. Chem. Int. Ed.*, 2009, **48**, 3914-3921.
- C. S. Hawes, R. Babarao, M. R. Hill, K. F. White, B. F. Abrahams and P. E. Kruger, *Chem. Commun.*, 2012, **48**, 11558-11560.

- 41 C. S. Hawes and P. E. Kruger, *RSC Advances*, 2014, **4**, 15770-15775.
- 42 C. S. Hawes and P. E. Kruger, *Dalton Transactions*, 2014, **43**, 16450-16458.
- 43 M. B. Peterson, S. P. Le-Masurier, K. Lim, J. M. Hook, P. Martens and A. M. Granville, *Macromol. Rapid Commun.*, 2014, **35**, 291-297.
- 44 J. H. Kim, M. Lee and C. B. Park, *Angew. Chem. Int. Ed.*, 2014, **53**, 6280-6280.
- 45 M. A. Rahim, H. Ejima, K. L. Cho, K. Kempe, M. Müllner, J. P. Best and F. Caruso, *Chem. Mater.*, 2014, **26**, 1645-1653.
- 46 H. Ejima, J. J. Richardson, K. Liang, J. P. Best, M. P. van Koeverden, G. K. Such, J. Cui and F. Caruso, *Science*, 2013, **341**, 154-157.
- 47 W. Scarano, H. Lu and M. H. Stenzel, *Chem. Commun.*, 2014, **50**, 6390-6393.
- 48 W. Scarano, H. T. T. Duong, H. Lu, P. L. De Souza and M. H. Stenzel, *Biomacromolecules*, 2013, **14**, 962-975.
- 49 J. Cui, Y. Yan, G. K. Such, K. Liang, C. J. Ochs, A. Postma and F. Caruso, *Biomacromolecules*, 2012, **13**, 2225-2228.
- 50 A. L. Laine and C. Passirani, *Curr. Opin. Pharmacol.*, 2012, **12**, 420-426.
- 51 A. Levina, A. Mitra and P. A. Lay, *Metallomics*, 2009, **1**, 458-470.
- 52 S. Kapitza, M. Pongratz, M. A. Jakupec, P. Heffeter, W. Berger, L. Lackinger, B. K. Keppler and B. Marian, *J. Cancer Res. Clin. Oncol.*, 2005, **131**, 101-110.
- 53 M. A. Jakupec, E. Reisner, A. Eichinger, M. Pongratz, V. B. Arion, M. Galanski, C. G. Hartinger and B. K. Keppler, *J. Med. Chem.*, 2005, **48**, 2831-2837.
- 54 B. M. Blunden and M. H. Stenzel, *Journal of Chemical Technology & Biotechnology*, 2015, **90**, 1177-1195.
- 55 C. Santini, M. Pellei, V. Gandin, M. Porchia, F. Tisato and C. Marzano, *Chem. Rev.*, 2014, **114**, 815-862.
- 56 T. W. Liu, T. D. MacDonald, J. Shi, B. C. Wilson and G. Zheng, *Angew. Chem. Int. Ed.*, 2012, **51**, 13128-13131.
- 57 C. J. Anderson and R. Ferdani, *Cancer Biother. Radiopharm.*, 2009, **24**, 379-393.
- 58 A. E. Hansen, A. L. Petersen, J. R. Henriksen, B. Boerresen, P. Rasmussen, D. R. Elema, P. M. a. Rosenschöld, A. T. Kristensen, A. Kjær and T. L. Andresen, *ACS Nano*, 2015, **9**, 6985-6995.
- 59 E. Gourni, L. Del Pozzo, E. Kheirallah, C. Smerling, B. Waser, J.-C. Reubi, B. M. Paterson, P. S. Donnelly, P. T. Meyer and H. R. Maecke, *Mol. Pharm.*, 2015, 10.1021/mp500671j.
- 60 P. Schumann, V. Collot, Y. Hommet, W. Gsell, F. Dauphin, J. Sopkova, E. T. MacKenzie, D. Duval, M. Boulouard and S. Rault, *Bioorg. Med. Chem. Lett.*, 2001, **11**, 1153-1156.
- 61 E. H. Vickery, L. F. Pahler and E. J. Eisenbraun, *The Journal of Organic Chemistry*, 1979, **44**, 4444-4446.
- 62 A. Postma, Y. Yan, Y. Wang, A. N. Zelikin, E. Tjijto and F. Caruso, *Chem. Mater.*, 2009, **21**, 3042-3044.
- 63 B. Yu, D. A. Wang, Q. Ye, F. Zhou and W. Liu, *Chem. Commun.*, 2009, **0**, 6789-6791.
- 64 S. Jens-Uwe and J. S. B. David, *Methods and Applications in Fluorescence*, 2014, **2**, 024005.
- 65 S. Hong, Y. S. Na, S. Choi, I. T. Song, W. Y. Kim and H. Lee, *Adv. Funct. Mater.*, 2012, **22**, 4711-4717.
- 66 Q. Liu, B. Yu, W. Ye and F. Zhou, *Macromol. Biosci.*, 2011, **11**, 1227-1234.
- 67 C. Zhao, F. Zuo, Z. Liao, Z. Qin, S. Du and Z. Zhao, *Macromol. Rapid Commun.*, 2015, **36**, 909-915.
- 68 Y. Yu, J. G. Shapter, R. Popelka-Filcoff, J. W. Bennett and A. V. Ellis, *J. Hazard. Mater.*, 2014, **273**, 174-182.
- 69 N. Farnad, K. Farhadi and N. Voelcker, *Water, Air, Soil Pollut.*, 2012, **223**, 3535-3544.

